J Mater Sci (2009) 44:6060–6068
DOI 10.1007/s10853-009-3833-9

Dielectric relaxation studies on [PEO–SiO_2]:NH_4SCN nanocomposite polymer electrolyte films

S. L. Agrawal · Markandey Singh · Mridula Tripathi · Mrigank Mauli Dwivedi · Kamlesh Pandey

Received: 8 May 2009 / Accepted: 21 August 2009 / Published online: 3 September 2009

Abstract Present work deals with findings on dielectric relaxation behaviour and a.c. conduction in a SiO_2-doped polymer nanocomposite electrolyte system, namely, $[(100 - x)\,PEO + x SiO_2]:y NH_4SCN$. The formation of nanocomposite has been ascertained by XRD measurements. The effect of salt and filler (SiO_2) on conductivity response of PEO-based nanocomposite polymer electrolyte has been investigated by impedance spectroscopy. The variation of dielectric permittivity, dielectric loss and modulus spectra with frequency and temperature was carried out from impedance spectroscopy data. The a.c. conductivity seems to follow the universal power law.

Introduction

The solid nanocomposite polymer electrolyte is a prominent class of electrolyte material for electrochemical device application, with properties of good thermal stability and high electrical conductivity, mechanical strength, flexibility, optical density, corrosion toughness, etc. Within the framework of nanocomposite polymer electrolyte, poly(ethylene oxide) PEO-based polymeric nanocomposite electrolytes are the most extensively investigated system because PEO has a single helical structure which supports fast ion transport [1–3]. Further, PEO has good complexation properties (high solvating behaviour), partial crystalline/amorphous nature, low melting point (65–69 °C) and glass transition temperature [1, 3, 4]. However, due to high crystalline phase concentration, the conductivity of PEO-based electrolyte is limited. This is mainly due to basic requirement for ionic conduction, viz. ionic motion coupled to the segmental motion (relaxation) of flexible amorphous polymer phases [5]. Different proton/anion conducting polymer electrolytes based on wide range of polymer hosts like poly(ethylene oxide) PEO, polyvinyl alcohol (PVA), polyethylene glycol (PEG), polymethylmethaacrylate (PMMA), polyvinylidene fluoride (PVdF) complexed with some ammonium salts (NH_4SCN, NH_4HSO_4, NH_4ClO_4, NH_4I, etc.) and acids (H_3PO_4, H_2SO_4 and HCl, etc.) have been developed over the years [6–10]. Various attempts have been made in the past decade to enhance the ionic and mechanical properties with the addition of different organic and inorganic fillers leading to formation of composite polymer electrolyte [CPE] [11, 12]. SiO_2, TiO_2, Al_2O_3, SnO_2, etc., are some of the inorganic inert fillers that have been tried to attain high ionic conductivity [13–15]. Scaling down of these inert inorganic fillers to nanometric size have been shown to improve significantly the ion conducting properties of these composite polymer electrolytes in the recent past [16–18].

Though such systems have evolved a great deal, it becomes important to understand the ion transport behaviour under dynamical conditions in these composite polymer

S. L. Agrawal · M. Singh
Department of Physics, A.P.S. University, Rewa, MP, India
e-mail: sla_ssi@rediffmail.com

M. Singh
e-mail: mk143singh@gmail.com

M. Tripathi
Department of Chemistry, C.M.P. Degree College, University of Allahabad, Allahabad, India
e-mail: mt68@rediffmail.com

M. M. Dwivedi · K. Pandey (✉)
National Centre of Exp. Mineralogy and Petrology, University of Allahabad, Allahabad 211002, India
e-mail: kp542831@gmail.com

M. M. Dwivedi
e-mail: mmdwivedi@gmail.com

electrolytes. Besides there is dearth of proton conducting electrolyte system with high ionic conductivity, thermal stability and mechanical stability for certain electrochemical devices like smart windows, sensors, etc. The ion transport property depends upon several factors like degree of salt dissociation, salt concentration, dielectric constant of host polymer, degree of ion aggregation and mobility of polymer chains. Further, ion association in a heterogeneous system is directly related to the presence of dipoles due to solvent dipoles/ion pairs [16, 19]. The dielectric properties of ion conducting polymer electrolyte provide valuable information even though these materials have sufficiently high ionic conductivity. Both dielectric relaxation and frequency dependent conductivity are sensitive to the motion of charged species of dipolar polymers. Thus, the study of dielectric relaxation phenomenon is a powerful tool to understand ion transport behavior and ionic/molecular interactions in solid polymer electrolytes [20, 21].

In view of the above, an innovative approach has been made to use nanosized SiO_2 material as filler in development of PEO–NH_4SCN-based nanocomposite polymer electrolyte and its electrical characterization in the present work. The structural aspect of electrolyte has been studied by XRD measurement technique. To explain the effect of salt or filler, in the enhancement of a.c. conductivity of solid polymer electrolyte under different conditions, the frequency- and temperature-dependent dielectric behaviour and a.c. conductivity have been investigated.

Experimental

Synthesis

Polyethylene oxide PEO (MW $\sim 6 \times 10^5$, ACROS Organics) and NH_4SCN salt, (Rankem India, AR grade) were used for the synthesis of composite electrolyte. The synthesis of nanosized ceramic filler (SiO_2) was carried out by a two-step sol–gel process [17]. The sol–gel developed solution was admixed stoichiometrically in PEO solution (in de-ionized water at 40 °C) and stirred for 10 h continuously. Subsequently, known amount of NH_4SCN salt was admixed in PEO–SiO_2 solution. This gelatinous polymeric solution was finally cast in polypropylene dishes. The solution cast film was finally dried at room temperature to obtain free standing films of CPE.

Characterization

Structural behavior of PEO–SiO_2 and PEO–SiO_2–NH_4SCN system and crystallite size of the electrolytes were studied by X-ray diffractometer (Phillips X-Pert model) in the Bragg's angle range (2θ) 15–60°. The electrical characterization of the solid polymer composite electrolyte was carried out using impedance spectroscopy on application of a small a.c. signal across the sample cell with Pt blocking electrodes. The complex impedance parameters were measured on an impedance analyzer (HIOKI LCR Hitester, model: 3522, Japan). The dielectric relaxation, modulus spectra and a.c. conductivity were derived from impedance spectroscopy data.

Result and discussion

Structural studies

The XRD pattern of PEO–SiO_2 and [PEO–SiO_2]:NH_4SCN for different composition systems are shown in Fig. 1. All the curves show the presence of background modulation, a feature prevalent in polymeric systems. In the XRD pattern, existence of broad peaks, in addition to few sharp

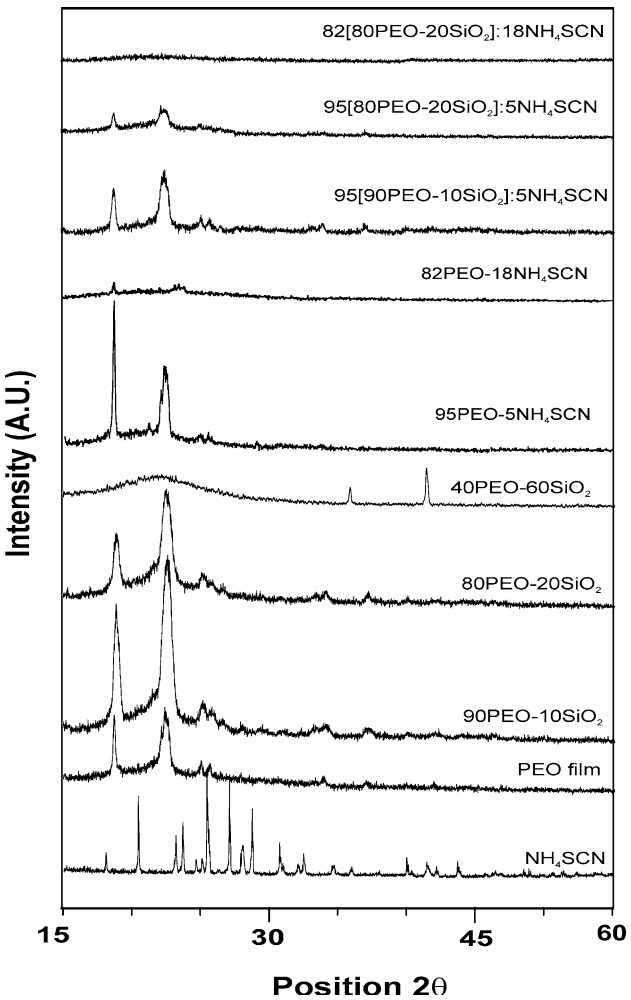

Fig. 1 The XRD patterns of different nanocomposite polymer electrolytes system

reflections, additionally confirms partially crystalline and amorphous nature of the electrolyte system. Doping of salt and filler in PEO host matrix give some important informations. Intercalation of polymer chain with ceramic filler (silica) usually increases the interlayer spacing of the filler. This effect leads to shift of diffraction peaks towards the lower 2θ value which are related through the Bragg's relation

$$2d \sin\theta = \lambda \text{ (for } n = 1) \quad (1)$$

Figure 1, clearly indicates that addition of ceramic filler (SiO_2) in polymer host (PEO) reduces the intensity of main peaks (in PEO, $2\theta = 19°$ and 23°) followed by broadening of the peak area, which is an indication of reduction in degree of crystallinity (When SiO_2 concentration exceeds 50 wt% in PEO:SiO_2, peaks get submerged in broadening and few new peaks of SiO_2 appear). From this diffractogram, it is also inferred that at lower weight percentage of SiO_2 (10 wt%),

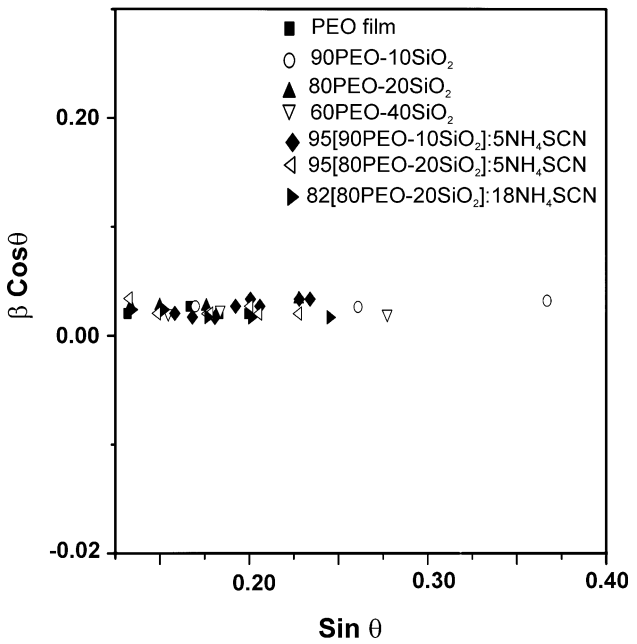

Fig. 2 Williamson–Hall plot of different nanocomposite polymer electrolytes

the crystallite size of silica is large but as SiO_2 concentration increases to 60 wt%, the dispersal becomes homogeneous followed by reduction in size. At higher ratio of SiO_2 (60 wt%) in polymer host, the peak of SiO_2 reappears due to cluster formation with reduction in crystallinity. It is interesting to note shift in diffraction maxima to lower 2θ value upon enhancement of SiO_2 concentration. The magnitude of shift varies with doping ratio. When salt is doped to form NCPE, no new peak appears; rather existing peaks of PEO:SiO_2 reappear at the same 2θ value but with reduced intensity. Samples with higher salt content give a completely amorphous film which suggests interaction of polymer with salt. The average crystallite size of crystallites when calculated by the well known Scherer's formula [22], yield a variation from 20 to 50 nm.

In order to distinguish the effect of crystallite-size-induced broadening and strain-induced broadening in FWHM of XRD profile, the Williamson–Hall plot method [23] was adopted. In this method, we calculate crystallite size (without strain) from sin θ versus β cos θ plot (shown in Fig. 2) in accordance with the following relation

$$\beta \cos\vartheta = \frac{C\lambda}{L} + 2\varepsilon \sin\vartheta \quad (2)$$

where β is FWHM and L is the grain size (nm), C the correction factor, ε the strain and λ the wavelength of X-ray beam. Table 1 also lists the crystallite size for PEO–SiO_2 and $[(100 - x)\text{PEO} + x\text{SiO}_2]:y\text{NH}_4\text{SCN}$ composite systems. This table thus ascertains nanometric dimension of synthesized electrolyte.

Dielectric studies

Figures 3 and 4 present the variation of dielectric permittivity (ε') and dielectric relaxation (ε'') as a function of frequency and temperature for as synthesized nanocomposites. The real and imaginary part of permittivity was calculated from the relation

$$\varepsilon^* = \varepsilon' - j\varepsilon'' \quad (3)$$

where $\varepsilon' = \frac{-Z''}{\omega C_0 (Z'^2 + Z''^2)}$ and $\varepsilon'' = \frac{Z'}{\omega C_0 (Z'^2 + Z''^2)}$

Table 1 Average particle size of undoped and doped PEO:SiO_2 film for different compositions calculated by different techniques

Sample	Calculated particle size (nm)	
	By Scherer's method	By W–H plot
1. Pure PEO	45.2	42.6
2. 90 wt% PEO + 10 wt% SiO_2 film	23.7	22.0
3. 80 wt% PEO + 20 wt% SiO_2 film	22.8	22.1
4. 40 wt% PEO + 60 wt% SiO_2 film	21.2	21.0
5. [90 wt% PEO + 10 wt% $SiO_2]_{95}$:$(NH_4SCN)_5$ film	32.5	26.5
6. [80 wt% PEO + 20 wt% $SiO_2]_{95}$:$(NH4SCN)_5$ film	25.7	25.0
7. [80 wt% PEO + 20 wt% $SiO_2]_{82}$:$(NH_4SCN)_{18}$ film	48.0	39.2

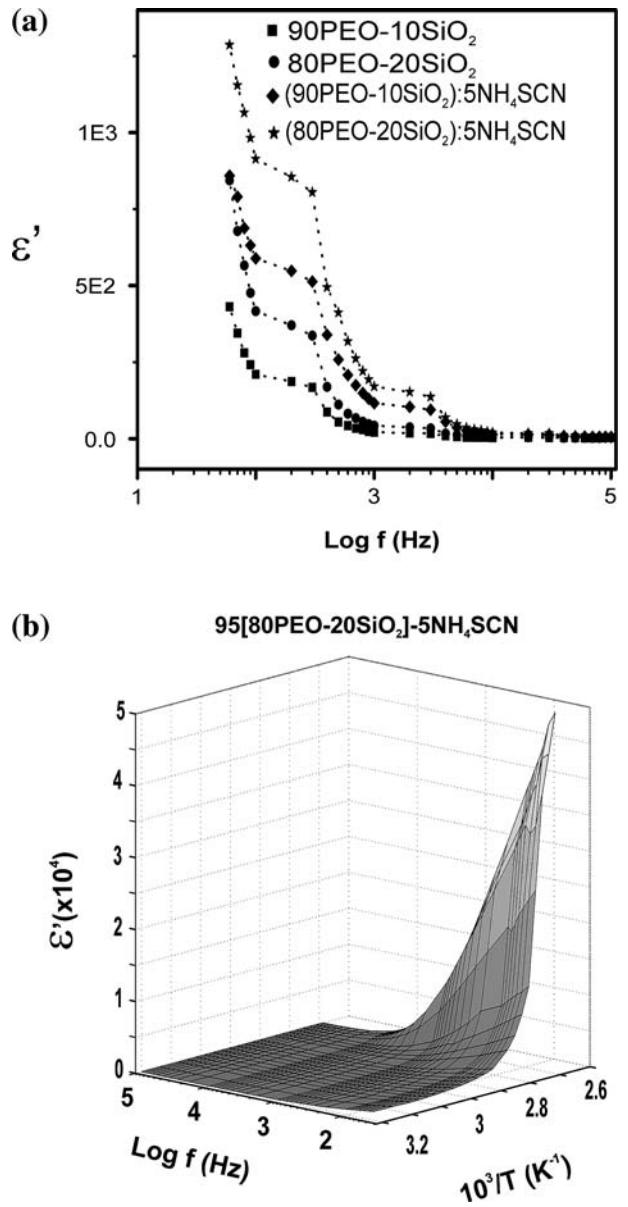

Fig. 3 **a** Variation of dielectric constant with frequency for different compositions. **b** Variation of dielectric constant with frequency and temperature for [80PEO–20SiO_2]:5NH_4SCN CPE system

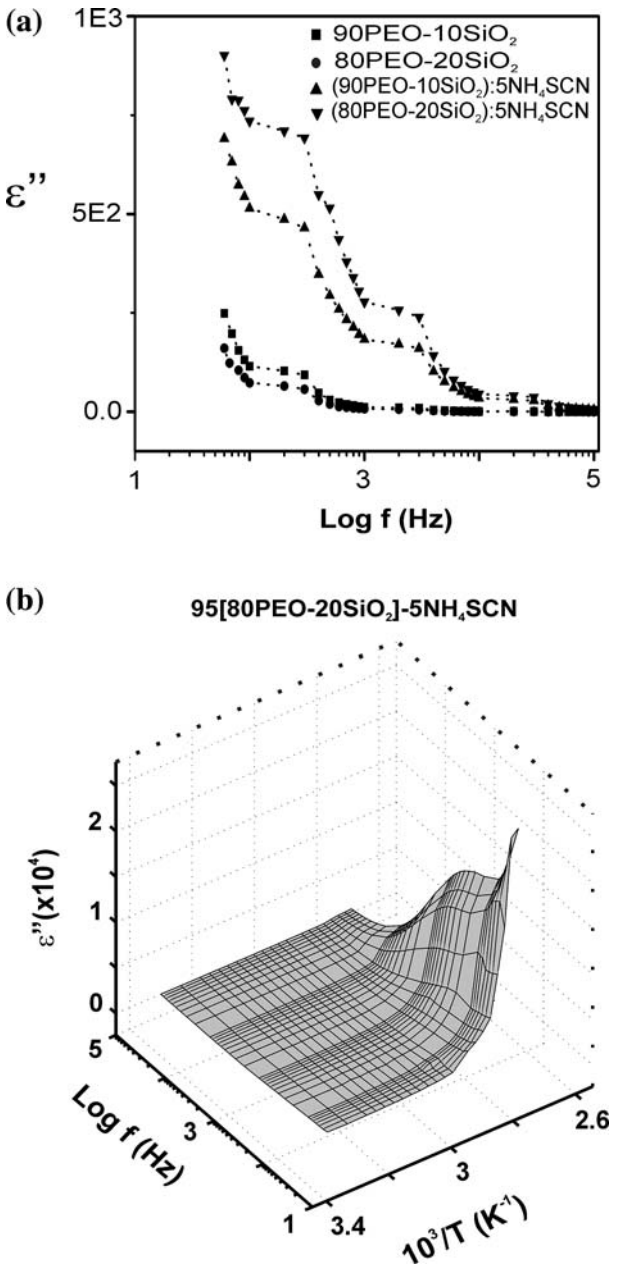

Fig. 4 **a** Variation of imaginary part of dielectric relaxation with frequency for different composition. **b** Variation of imaginary part of dielectric relaxation with frequency and temperature for [80PEO–20SiO_2]:5NH_4SCN CPE system

Figures 3a and 4a show the variation of ε' and ε'' with frequency for two different composition of the [$(100 - x)$ PEO $- x$$SiO_2$] composites and [$(100 - x)$PEO $+ x$$SiO_2$]:$y$$NH_4$SCN composite electrolyte films. In both the cases a strong frequency dispersion in dielectric permittivity (ε') was recorded in low frequency region followed by a nearly frequency-independent nature in the high frequency regime (above 10 KHz)—a typical feature of polymeric substances [24]. Similar observation was also recorded in the imaginary part of dielectric permittivity shown in Fig. 4a. The decrease of ε' and ε'' with increasing frequency may be attributed to electrical relaxation or inability of dipoles to rotate rapidly leading to a lag between frequency of oscillating dipoles and that of applied field. As the frequency increases, the ionic and orientational source of polarizability decreases and finally disappears due to inertia of mobile ions to result in a nearly constant value of dielectric permittivity. Interestingly, dispersion at lower frequencies seems to be higher in case of composite electrolyte. This is possibly due to suppression of large-scale heterogeneity in pristine complex and its replacement with

small-scale heterogeneity. The small-scale heterogeneity is related to presence of silica which increases the volume on account of looser segmental packing of chains [25]. Another important fact noticed in Figs. 3a and 4a is the appearance of two peaks, one in the frequency range 100–400 Hz and the other around 2 KHz at room temperature. In low-frequency region, charge accumulation at interface lead to a net polarization resulting in formation of space charge region at electrode–electrolyte interface. This material electrode interfacial polarization is possibly the reason for the occurrence of permittivity/relaxation peak in the low-frequency (100–400 Hz) range which has masked the other relaxation processes. The second peak through linear dispersion can be attributed to the dielectric relaxation phenomenon and the so-called β-relaxation peak in polyethylene oxide. This peak is associated with an amorphous transition involving short-range bond rotation. This inference is based on the fact that PEO exhibits three type of relaxations [26] designated as α, β and γ transitions. The α relaxation is observed close to the melting point of PEO ($T_m \sim 70$ °C) and attributed to motion of the chains associated with the crystalline phase [27]. The β-relaxation is usually detected in the range 250–300 K and associated with local motion of chain segments or side group.

Addition of salt (NH_4SCN) in PEO–SiO_2 to form electrolyte system may result in more localized charge carriers along with the mobile ions causing enhancement in dielectric permittivity/dielectric relaxation around 2 kHz frequency. This is in agreement with investigation of Wintersgill and Fontanella [28] and Gray [29] concerning the permittivity of salt in PEO or PPG systems. This behaviour is most likely caused by changes in the average dipole moment or the polarizibility of the solvent due to the dissolution of salt.

Figures 3b and 4b also show the variation of dielectric permittivity (real and imaginary part respectively) at different temperatures where the dielectric permittivity/dielectric loss is seen to increase with increasing temperature. The observed behaviour can be explained if the system is assumed to be formed of molecular dipoles. These dipoles remain frozen when the temperature is low. As the temperature increases, the dipoles become more thermally activated, having more rotational freedom, which leads to the observed increase in the dielectric parameter [30]. It is inferred that all types of polarization, except for thermally activated space charge polarization, will contribute to the dielectric polarization response in the low-temperature range. On the other hand, at high temperatures beyond the melting temperature of polymer host, the thermally activated space charge will contribute to the polarization process, which leads to the observed increase in ε' & ε'' and the dispersion process. The entire response reflects a non-Debye type relaxation in the composite electrolyte system.

Relaxation process in ionic conductors can also be well described by dielectric tangent loss (tan δ) which is defined as

$$\tan\delta = \varepsilon''/\varepsilon' \quad (4)$$

The variation of loss tangent (tan δ) with frequency and temperature for different compositions of PEO:SiO_2 and corresponding electrolytes containing 5 wt% NH_4SCN are shown in Fig. 5. The composition-dependent curve (Fig. 5a) of tangent loss shows no clear peak in the

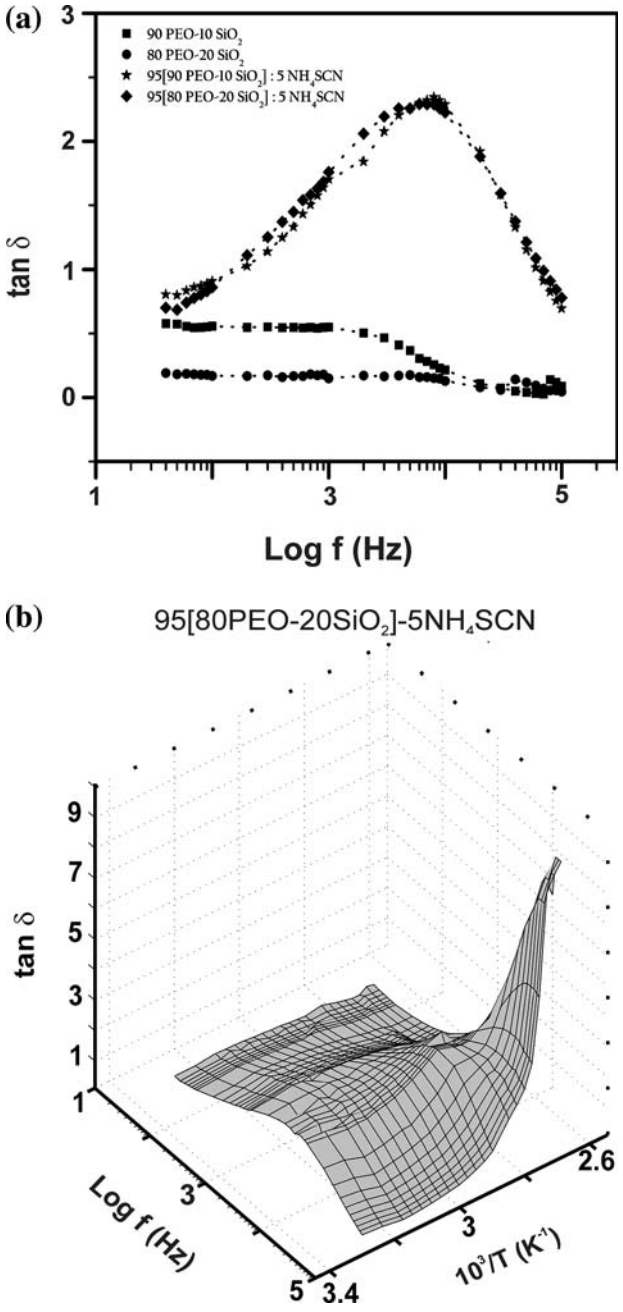

Fig. 5 **a** Variation of dielectric loss tangent (tan δ) with frequency for different composition. **b** Variation of dielectric loss tangent (tan δ) with frequency and temperature for [80PEO–20SiO_2]:5NH_4SCN CPE system

$(100 - x)$PEO $- x$$SiO_2$ films, rather a slope change is observed in 2000–3000 Hz frequency range. Essentially such a step change corresponds to occurrence of a broad peak which symptomizes the presence of scaling dipoles and related to β relaxation of PEO. Presence of relaxation dipoles may be due to the orientation of polar groups present in the side group of the polymer. This type of relaxation is called the dipolar group relaxation. Further loss peak is seen to shift to lower frequency with increase of SiO_2 content. This reaffirms our earlier result that enhancement in SiO_2 content loosens the segmental packing in chain thereby increasing the free volume for dipolar relaxation. When NH_4SCN is admixed in PEO–SiO_2 system to form NCPE a well-defined peak (sharper with respect to PEO–SiO_2) sets in. Such behavior can be successfully explained in terms of dielectric relaxation process associated with the presence of heterogeneities in the sample matrix. XRD studies have shown that addition of salt enhance the amorphosity of polymer electrolyte film. Thus this peak can be attributed to segmental diffusion motion in amorphous region. In the amorphous region, the network structure is expected to form more effectively. The doping of salt changes the amorphosity and produce relatively fast segmental motion coupled with mobile ion. As a consequence, a well-defined peak appears at relatively higher frequencies for NCPE films in the tan δ versus frequency curve. Asymmetry in peak has been observed in this plot for NCPE. This is possibly due to merger of more than one relaxation and indicative of non-Debye relaxation behaviour. This change of tan δ with frequency and temperature for a system 95[80PEO–20SiO_2]:5[NH_4SCN] is given in Fig. 5b. Figure 6 shows the temperature dependence of relaxation time. Though the variation of ln τ with respect to $1/T$ broadly suggest a Debye type relaxation process, careful examination of curve, suggests non-Arrhenius type behaviour of relaxation time and hence can be best described by VTF type relationship

$$\ln \tau = \ln \tau_0 - B/T - T_0 \quad (5)$$

where τ is the relaxation time at temperature T, τ_0 is the limiting value of relaxation time, T_0 the equilibrium glass transition ($T_g - 50 = T_0$) and B is a constant corresponding to activation energy of relaxation. The limiting value of relaxation time from Fig. 6 was obtained as 2.5×10^{-4} s. According to Eyring and coworkers [31], the relation between the relaxation time and ambient temperature can be obtained by using the following formula [32].

$$\tau = (h/KT)\exp(\Delta F/RT) \quad (6)$$

where h is the Planck's constant, R the universal gas constant and ΔF the free energy of activation. For 95[80PEO–20SiO_2]:5NH_4SCN system, the value of free energy of activation varies in between 6.15 and 7.02 kcal/mole from room temperature to 100 °C.

A plot of dielectric intensity log $\Delta\varepsilon'$ (where $\Delta\varepsilon'$ is the difference between the dielectric constant at any temperature and that at room temperature) versus the reciprocal of ambient temperature at fixed frequency is shown in Fig. 7. This curve is once again best described by Vogel–Tamman–Fulcher (VTF) law in the low-temperature regime. At high temperature, i.e., beyond melting temperature of host polymer Arrhenius behaviour is recorded. The activation energy

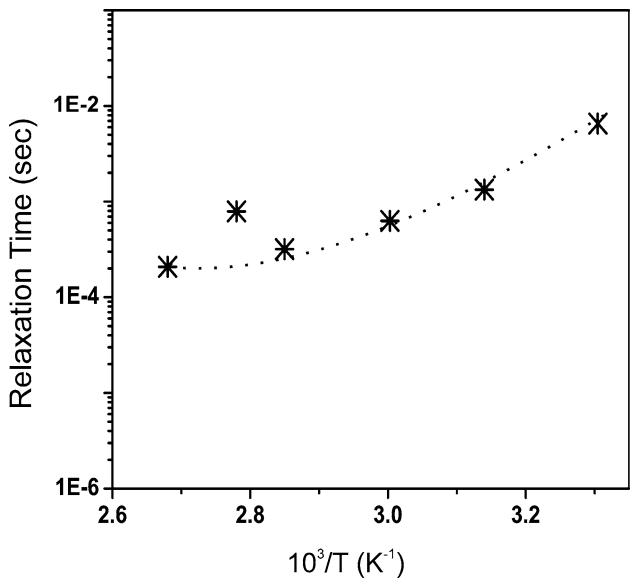

Fig. 6 Temperature dependent of relaxation time (τ) for 95[80PEO–20SiO_2]:5NH_4SCN polymeric electrolytes film

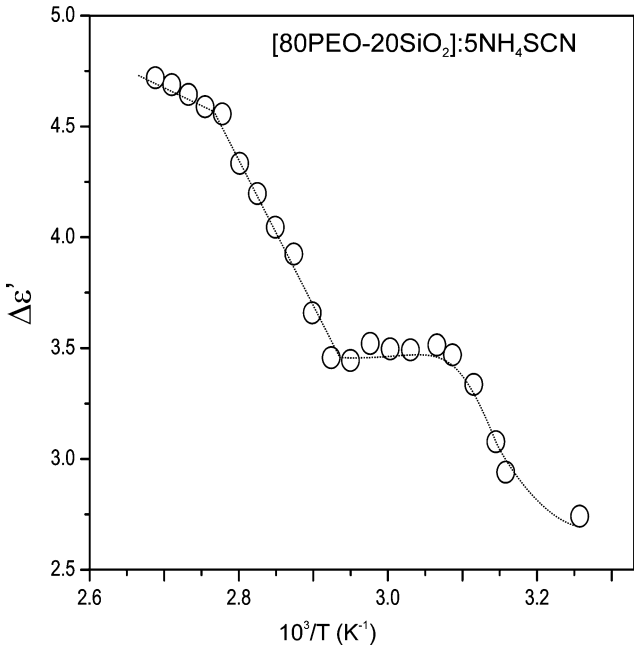

Fig. 7 Temperature dependent of $\Delta\varepsilon'$ for 95[80PEO–20SiO_2]:5NH_4SCN CPE at various frequencies

of the sample beyond 70 °C decreases as the temperature increases. This region corresponds to melting region of host polymer PEO [14, 17] and so related to structural transition. Around the structural transition region this tends to cause step difference in the presence of field. Beyond 70 °C thermally activated Debye process starts dominating and so the strength of polarizibility again enhances.

To study the electrode effect in the system, we have analyzed the dielectric spectra by complex electric modulus $M^*(\omega)$ [33, 34]. The complex electric modulus can be evaluated from the following relations.

$$M^*(\omega)\varepsilon'(\omega) = 1 \tag{7}$$

where $M^*(\omega) = M'(\omega) + iM''(\omega)$; $M'(\omega) = \varepsilon'(\omega)/\varepsilon'(\omega)^2 + \varepsilon''(\omega)^2$ and $M''(\omega) = \varepsilon''(\omega)/\varepsilon'(\omega)^2 + \varepsilon''(\omega)^2$.

Figure 8a, c shows the real and imaginary part of dielectric modulus versus log (frequency) spectra plotted at different temperatures (RT to 100 °C) for 95[80PEO–$20SiO_2$]:$5NH_4SCN$ polymeric system. The plots M' and M'' with log f show features of ionic conduction and S-shaped dispersion in M' and a peak in M'' in higher frequency range [35]. In the modulus formalism, the electrode polarization effect seems to clearly vanish in contrast to the dielectric formalisms where it is observed around 300 Hz. In Fig. 8c the peak is assumed to be related to the translational ion dynamics and mirrors the conductivity relaxation of mobile ions. The shape of the spectrum is identical for all temperatures and shows a single relaxation peak in the range of temperature and frequency determined. The maxima in these spectra occurs at $\omega_m = 1/\tau$, where τ is the relaxation time [36]. In these figures it is noticed that a long tail at low frequency is due to the large capacitance associated with electrolytes.

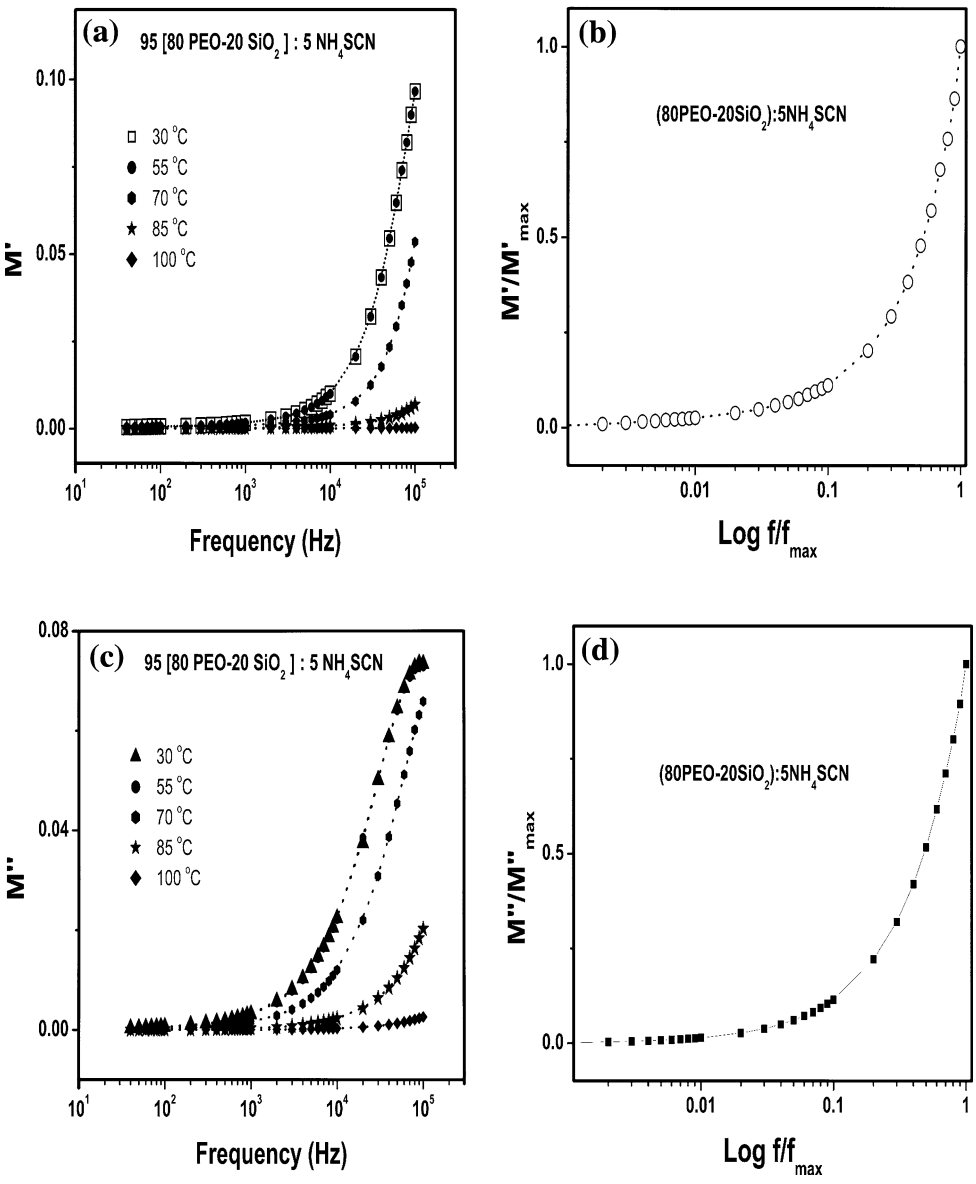

Fig. 8 Variation of **a** real part of electric modulus (M') with frequency at different temperature, **b** normalize M' with normalize frequency, **c** imaginary part of electric modulus (M'') with frequency at different temperature and **d** normalize M'' with normalize frequency

The broad and asymmetrical shape of electric modulus is generally described by the stretched exponential function of the electric field as [37].

$$\Phi(t) = \exp[(-t/\tau)^{\beta}] \quad (8)$$

where $0 < \beta < 1$ is an exponent indicating departure from the Debye relaxation ($\beta = 1$) and τ is the relaxation time. The variation of M' and M'' with frequency shows that the relaxation frequency is obtained easily in higher temperature regime but the shape of curve remains constant. Similarly, the frequency of modulus maximum M''_{max} shifts to higher frequency side with increase in temperature. It is also observed that M'' spectra at any particular temperature do not merge into a single master curve for various compositions. This indicates that the relaxation dynamics varies with salt composition [38].

The scaling behaviour of the real and imaginary part of electric modulus was also examined. The M' and M'' spectra are scaled by M'_{max} and M''_{max}, respectively. Frequency axis is scaled by relaxation frequency. The scaled (normalized) behaviour of M' and M'' with f/f_{max} is presented in Fig. 8b, d. These plots show non-symmetric nature, which suggests a distribution of relaxation time for the relaxation process [39].

The variation of a.c. conductivity with frequency for different composition is shown in Fig. 9. The a.c. conductivity (σ_{ac}) is calculated from the data on dielectric constant (ε') and tan δ using the relation.

$$\sigma_{ac} = \varepsilon' \varepsilon_0 \omega \tan \delta \quad (9)$$

where ε_0 is the vacuum permittivity and ω the angular frequency. It is apparent from Fig. 9 that ac conductivity

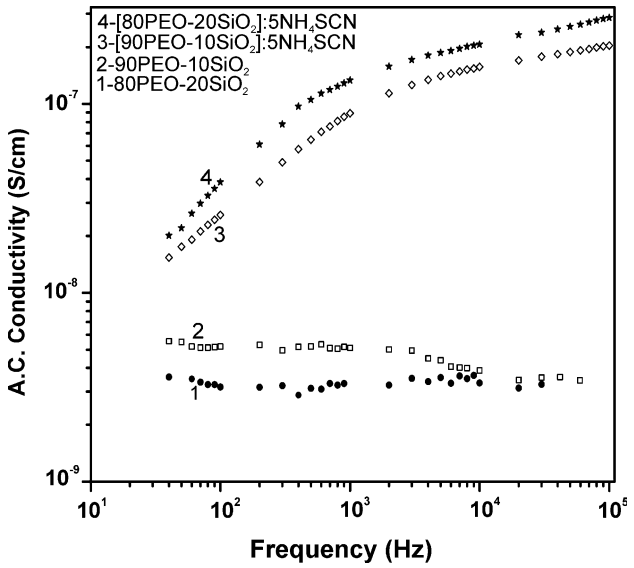

Fig. 9 Variation of a.c. conductivity with frequency for different polymer composite electrolyte systems

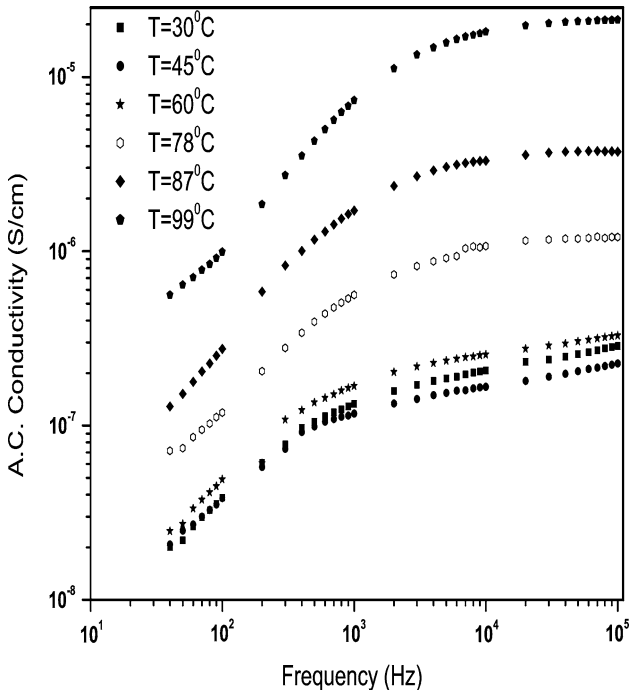

Fig. 10 Variation of a.c. conductivity of 95[80PEO–20SiO_2]:5NH_4SCN film with frequency at different temperatures

roughly remains constant with frequency. In ambient, after doping of salt (NH_4SCN), the conductivity increases linearly up to 2 kHz and thereafter the increase tends to settle down and show a small plateau. From Fig. 10, it can be assumed that the a.c. conductivity (σ_{ac}) of the samples depend on the frequency (ω) according to the well-known power law [40].

$$\sigma_{ac} = A\omega^{p} \quad (10)$$

where A is a constant and p is the frequency exponent ($p < 1$). The ω^p power law is very frequently observed in a wide range of materials among which is polymer. It is also observed that the increase in filler content enhances a.c. conductivity. The calculated value of power law exponent (p), generally for ionic conductor can be between 1.0 and 0.5, indicating the ideal long-range pathway diffusion limited hopping [41]. If $p = 0$ the motion is completely random and independent Debye like ion hops. In the present case p was found to be 0.7. A physical model (i.e., jump relaxation model) has been developed for structurally disordered ionic conductors [42] in order to rationalize the observed frequency dispersion since the dynamical effects of polymer host due to the segmental renewing rates become less significant below microwave region. According to jump relaxation model, at very low frequencies ($\omega \rightarrow 0$) an ion can jump from one site to its neighboring vacant site successfully contributing to the dc conductivity. At higher frequencies, the probability for the ion to go back again to its initial site increases due to the short

time periods available. The high probability for the correlated forward–backward hopping at higher frequencies together with the relaxation of the dynamic cage potential is responsible for the observed high frequency conductivity dispersion. It has been observed that the maximum value of conductivity is 3.0×10^{-7} S cm^{-1} for 5 wt% NH_4SCN concentration.

Conclusions

In [PEO–SiO_2]:NH_4SCN nanocomposite polymer electrolyte, XRD study showed that addition of ceramic filler and salt reduced the crystallinity. This also confirms the average particle size in the film to be in nanosize format. The variation of relative dielectric constant with frequency shows the presence of material electrode interface polarization process. It also indicates that ionic and polymer segmental motion is strongly coupled. The effect of salt addition rather than filler is more prominent in the variation of dielectric constant with frequency. The loss tangent peaks appearing at a characteristic frequency suggests the presence of relaxing dipoles in all the samples. The temperature dependence of the relaxation time shows a non-Arrhenius nature. The a.c. conductivity of the system follows Universal Power law behaviour.

References

1. Gray FM (1991) Solid polymer electrolyte: fundamental and applications. VCH, New York
2. Scrosati B (1993) Applications of electroactive polymer. Chapman and Hall, London
3. Bruce PG, Grey F, Shriver DF (1995) In: Bruce PG (ed) Solid state electrochemistry. Cambridge University Press, Cambridge, UK
4. Wieczorek W, Raducha D, Zalewska A, Stevens JR (1998) J Phys Chem B 102:8725
5. Daniel MF, Desbat B, Lassegues JC (1988) Solid State Ionics 28:632
6. Hashmi SA, Kumar A, Maurya KK, Chandra S (1990) J Phys D Appl Phys 23:1307
7. Agrawal SL, Shukla PK (2000) Ind J Pure Appl Phys 38:53
8. Binesh N, Bhatt SV (1996) Solid State Ionics 86–88:609
9. Donoso P, Gorecki W, Bertheir C, Defdini F, Poinsignon C, Armand MB (1988) Solid State Ionics 28:969
10. Pandey S, Shukla PK, Agrawal SL (2008) In: Chowdari BVR, Kulkarni AR, Suthanthiraj A, Nalini B, Kalaiselvi N, Harikumar G (eds) Solid State Ionics, New materials for pollution free energy devices, p 627
11. Wieczorek W, Florjaniczyk Z, Stevens JR (1995) Electrochim Acta 40:2251
12. Shukla PK, Agrawal SL (2000) Ionics 6:312
13. Kumar B (2004) J Power Sources 135:215
14. Chandra A, Srivastava PC, Chandra S (1995) J Mater Sci 30:3633. doi:10.1007/BF00351877
15. Pandey GP, Hashmi SA, Agrawal RC (2008) Solid State Ionics 179:543
16. Rajendran S, Sivakumar M, Subadevi R, Wu NL, Lee JY (2007) J Appl Polym Sci 103:3950
17. Pandey K, Dwivedi MM, Tripathi M, Singh M, Agrawal SL (2008) Ionics 14:515
18. Croce F, Persi L, Scrosati B, Serraino-Fiory F, Plichta E, Hendrickson MA (2001) Electrochim Acta 46:2457
19. Castillo J, Chacon M, Castillo R, Vargas RA, Bueno PR, Vasela JA (2009) Ionics. doi:10.1007/p 11581-009-0320-x
20. Kremer F, Schonhals A (2003) Broad band dielectric spectroscopy. Springer-Verlag, Berlin
21. Chand N, Jain D (2004) Bull Mater Sci 27:227
22. Cullity BD (1978) Element of X-ray diffraction, 2nd edn. Anderson-Wesley, London
23. Williamson GK, Hall HW (1953) Acta Metall 1:22
24. Awadhia A, Patel SK, Agrawal SL (2006) Prog Cryst Growth Charact Mater 52:61
25. Kanapitsas A, Pissis P, Kotsilkova R (2002) J Non-Cryst Solids 305:204
26. McCrum NG, Read BE, Williams G (1967) Anelastic and dielectric effects in polymeric solids. John Wiley and Sons, New York
27. Ohta Y, Yasuda HJ (1994) Polym Sci Part B: Polym Phys 32:2241
28. Wintersgill MC, Fontanella JJ (1989) In: McCallum JR, Vincent CA (eds) Polymer electrolyte reviews-2. Elsevier Applied Science, New York
29. Gray FM (1991) Solid polymer electrolyte, fundamental and applications. VCH, New York
30. Eyring H (1953) J Chem Phys 4:633
31. Glasston S, Laidler KJ, Eyring H (1941) The theory of rate process. McGraw Hill, New York, p 544
32. Senturk E (2004) J Solid State Chem 177:1508
33. Moynihan CT, Boesch LP, Bose R (1973) Phys Chem Glasses 14:122
34. Elliot SR (1994) J Non-Cryst Solids 170:97
35. Richter H, Wagner H (1998) Solid State Ionics 105:167
36. Ghosh S, Ghosh A (2002) J Phys: Condens Matter 14:2531
37. Hodge IM, Ngai KL, Moynihan CT (2005) J Non-Cryst Solids 351:104
38. Williams G, Watts DC (1971) Trans Faraday Soc 67:1322
39. Ross Macdonald J (2004) J Appl Phys 95:1849
40. Jonscher AK (1983) Dielectric relaxation in solids. Chelsea Dielectric Press, London
41. Gupta V, Man Singh A (1984) Phys Rev B 49:1989
42. Funke K (1992) Prog Solid State Chem 22:111